Graphene-Based Chemiluminescence Resonance Energy Transfer for Homogeneous Immunoassay

Joon Seok Lee,[†] Hyou-Arm Joung,[‡] Min-Gon Kim,[‡,*] and Chan Beum Park[†,*]

[†]Department of Materials Science and Engineering, Korea Advanced Institute of Science and Technology (KAIST), 335 Science Road, Daejeon 305-701, Korea, and [‡]Advanced Photonics Research Institute and Graduate Program of Photonics and Applied Physics, Gwangju Institute of Science and Technology, Gwangju 500-712, Korea

ABSTRACT

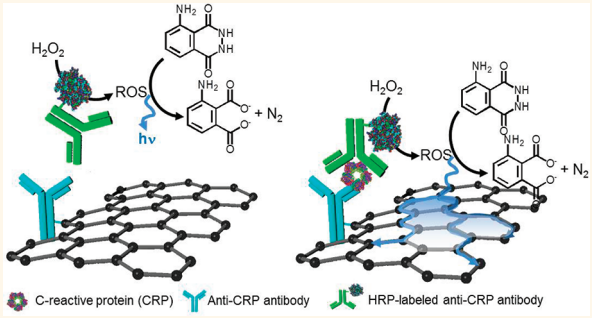

We report on chemiluminescence resonance energy transfer (CRET) between graphene nanosheets and chemiluminescent donors. In contrast to fluorescence resonance energy transfer, CRET occurs *via* nonradiative dipole–dipole transfer of energy from a chemiluminescent donor to a suitable acceptor molecule without an external excitation source. We designed a graphene-based CRET platform for homogeneous immunoassay of C-reactive protein (CRP), a key marker for human inflammation and cardiovascular diseases, using a luminol/hydrogen peroxide chemiluminescence (CL) reaction catalyzed by horseradish peroxidase. According to our results, anti-CRP antibody conjugated to graphene nanosheets enabled the capture of CRP at the concentration above 1.6 ngmL^{-1}. In the CRET platform, graphene played a key role as an energy acceptor, which was more efficient than graphene oxide, while luminol served as a donor to graphene, triggering the CRET phenomenon between luminol and graphene. The graphene-based CRET platform was successfully applied to the detection of CRP in human serum samples in the range observed during acute inflammatory stress.

KEYWORDS: graphene · chemiluminescence · CRET · immunosensors · C-reactive protein

Graphene nanosheet, a two-dimensional and zero band gap carbon crystal with a single atomic layer, has recently attracted much attention as a fascinating nanomaterial because of its unique structural, mechanical, and electronic properties, as well as the possibility of versatile applications.[1−5] In particular, the high specific surface area and biocompatibility of graphene can provide a suitable and promising platform for biological applications, such as drug delivery, biomarker detection, biomineralization, and electrochemical biosensing.[6−9] More recently, through photophysical calculations, graphene was predicted to be an excellent energy acceptor, with long-range energy transfer due to its extraordinary electronic properties.[10,11] The rate of the nanoscale, long-range resonance energy transfer was suggested to have a d^{-4} dependence on distance, in striking contrast to a d^{-6} dependence predicted from traditional fluorescence resonance energy transfer (FRET).[12,13] Liu *et al.* applied fluorescence quenching to the π system of graphene from excited electronic states of a fluorescent dye to a FRET system for biomolecular recognition.[14] As in the general fluorescence techniques, however, FRET suffers from drawbacks such as the requirement of simultaneous external excitation of both donor and acceptor fluorophores.[15−17]

Here we report on an immunosensing platform based on chemiluminescence resonance energy transfer (CRET) between graphene and chemiluminescent donors. CRET is a nonradiative dipole–dipole transfer of energy from a chemiluminescent donor to a suitable acceptor molecule.[17] In contrast to FRET, CRET occurs *via* the specific oxidation of a luminescent substrate during chemiluminescence (CL) reaction without an external excitation source; thus, it can avoid the above-mentioned drawbacks of FRET.[17] We designed a graphene-based CRET platform for homogeneous immunoassay, as illustrated in Figure 1. We used a luminol/hydrogen peroxide CL reaction catalyzed by horseradish peroxidase (HRP), which is one of the most sensitive and reliable CL reactions, used for many biological applications.[18] The reaction of luminol with ROS (*i.e.*, reactive oxygen

* Address correspondence to parkcb@kaist.ac.kr, mkim@gist.ac.kr.

Received for review November 8, 2011 and accepted March 14, 2012.

Published online March 14, 2012
10.1021/nn300684d

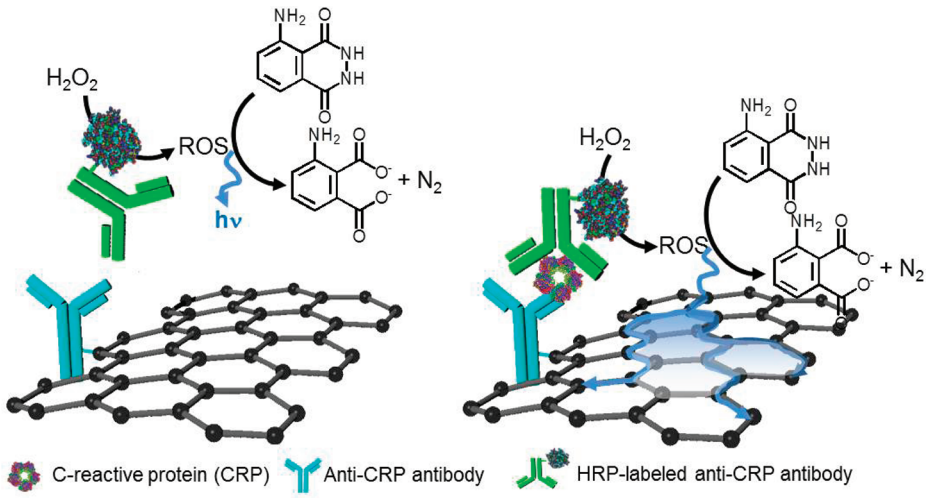

Figure 1. Schematic illustration of a graphene-based chemiluminescence resonance energy transfer platform for the detection of C-reactive protein (CRP). Anti-CRP antibody-conjugated graphene and luminol that is excited by horseradish peroxidase (HRP)-catalyzed oxidation are used as an acceptor and a donor, respectively.

species) such as singlet oxygen, which are generated by the reaction of hydrogen peroxide with HRP, results in the formation of a high energy species that decomposes with loss of nitrogen to give an excited molecule with a strong blue emission at 430 nm. We used C-reactive protein (CRP) as a model analyte for biomolecular recognition in this work. CRP, a hepatocyte-derived acute-phase protein, plays a key role in human inflammation and cardiovascular diseases.[19]

RESULTS AND DISCUSSION

For the construction of a graphene-based CRET immunosensor, we prepared bare graphene sheets by converting graphene oxide (GO) obtained from graphite powders through hydrothermal deoxygenation, using the modified Hummers method.[20] According to UV absorbance spectroscopic analysis (Figure S1 in Supporting Information), the typical band for GO with a maximum at 230 nm gradually red-shifted to around 267 nm after the hydrothermal reduction process owing to n $\rightarrow \pi^*$ transitions of aromatic C=C bonds. This indicates the restoration of the electronic conjugation within graphene and the excitation of the π-plasmon of the graphitic structure.[21] To enhance water solubility and avoid irreversible agglomeration during the immobilization of anti-CRP antibody, we further functionalized the surface of graphene with sulfonic acid groups.[22] The peaks at 1036, 1121, and 1170 cm^{-1} observed in the FT-IR spectrum (Figure S2) indicate characteristic vibrations of a sulfonated graphene surface.[22] The peak at 1727 cm^{-1} indicates that a carboxyl group and carbonyl moiety were still present on the edge of graphene surface after the reduction and sulfonation of GO, which could bind to amine groups in biomolecules.[14,22,23] We synthesized anti-CRP antibody-conjugated graphene nanosheets *via* a carbodiimide-assisted covalent reaction using *N*-ethyl-*N*′-(3-dimethylaminopropyl)carbodiimide (EDC) as a coupling agent and *N*-hydroxysuccinimide (NHS) as an activator. The NHS-activated carboxyl group on the edge of the graphene surface binds with the amine group of anti-CRP antibodies, resulting in the formation of an amide bond. According to the topographical profiles analyzed by atomic force microscopy (Figure 2), the height of the bare GO sheets was approximately 0.9 nm, which confirms a monolayer state of graphene sheets, while that of the dried anti-CRP antibody was 3.5 nm. After the immobilization of anti-CRP antibodies to NHS-activated graphenes, the antibody-conjugated graphene nanosheets exhibited brighter spots with increased heights (~4.5 nm) on their surfaces. We further investigated the anti-CRP antibody-conjugated graphene using circular dichroism (CD) spectroscopy. The CD spectrum of free anti-CRP antibody in a phosphate buffer solution showed a major negative peak at 215−220 nm, which is in good agreement with the CD spectrum of crystallized IgG antibody in the literature.[24] We could not observe any noticeable peak for bare graphenes (Figure S3). The CD spectrum of anti-CRP antibody−graphene conjugates exhibited characteristic bands similar to that of a free anti-CRP antibody (Figure S3), which implies that the secondary structure of the conjugated anti-CRP antibodies was retained on graphene surface.

To confirm the effectiveness of graphene as an acceptor in CRET before employing a sandwich-type CRET system, we investigated CRET by adding a different amount of NHS-activated graphene (or GO) to a reaction solution containing *free* HRP in excess. In the experiment, with the increasing amount of added NHS-activated graphene, the amount of free HRPs in the reaction solution should decrease because free HRPs become immobilized onto the NHS-activated graphene surfaces. After adding BSA for blocking the

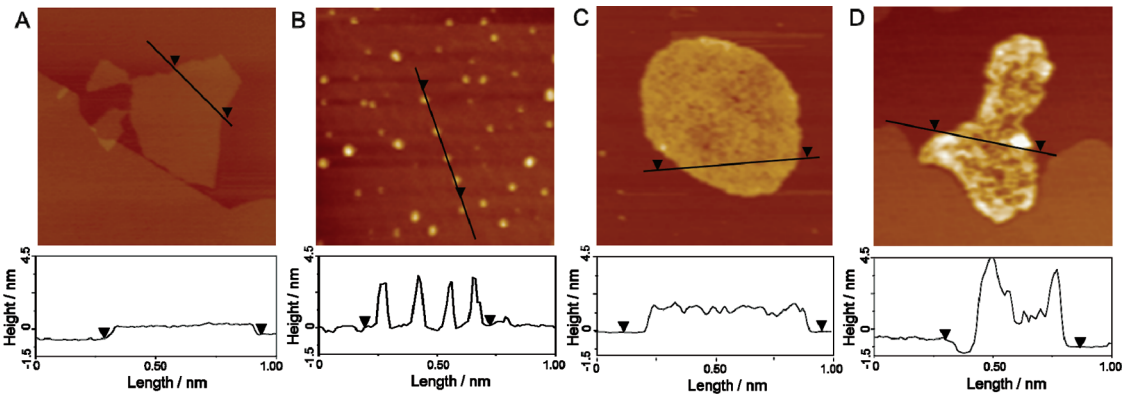

Figure 2. AFM images and height profiles of (A) bare graphene oxide, (B) anti-CRP antibodies, (C) sulfonated, water-soluble graphene, and (D) anti-CRP antibody-conjugated graphene on freshly cleaved mica. The antibody-conjugated graphene nanosheets exhibited brighter spots with increased heights (~4.5 nm) on their surfaces.

residual NHS moiety, we mixed the reaction solution with luminol and hydrogen peroxide. Then, we observed a gradual quenching of blue CL of luminol with the increasing amount of the NHS-activated graphenes, as shown in Figure 3A. The degree of CL quenching at 430 nm reached approximately 91% with 20 μg mL^{-1} NHS-activated graphenes. The CL quenching was well correlated to the relative concentration of HRP immobilized on the graphene, which was due to more acceptors (*i.e.*, graphene) combined with HRP brought closer to donors (*i.e.*, luminol excited by HRP-catalyzed oxidation), reaching a spacing suitable for CRET, thus, in turn, enabling higher energy transfer from the donor to the acceptor and more quenching of luminol CL. We carried out a control experiment without HRP conjugation using a HRP solution simply mixed with bare graphene to test the effect of proximity between graphene and HRP on CRET efficiency. As shown in Figure S4, the CL intensity of luminol in the control experiment remained almost unchanged even with the increased amount of graphene. This indicates that the proximity of HRP to graphene is critical for efficient energy transfer to graphene from excited luminol. We also investigated GO in comparison with graphene as an acceptor on CRET efficiency (Figure 3B). The maximum quenching efficiency of luminol was only 36% in the NHS-activated GO system at 20 μg mL^{-1}, which indicates that graphene is a more suitable acceptor for CRET than GO. As shown in Figure S1, there was a broad absorption across the visible spectrum of graphene (and GO), which overlaps with the chemiluminescence spectrum of luminol at around 430 nm. The spectral overlapping resulted in the CL quenching following an energy transfer mechanism.[25,26] However, the transfer of electrons from the excited state of luminol to graphene, a conductor that has a high electron transport property, should be much easier than that to GO, an insulator or semiconductor. According to literature,[27] fluorescence quenching is a nonradiative relaxation of excited electronic states to a ground state, which occurs by either energy transfer or photoinduced electron transfer in association with the properties of the fluorophore, local environment, and conjugation mode. Electron transport efficiency between graphite materials and excited dyes is a key factor for fluorescence quenching that is induced by interfacial charge transfer.[27,28]

On the basis of the above results, we applied graphene-based CRET to CRP detection using a sandwich-type interaction between anti-CRP antibody-conjugated graphene and an HRP-labeled anti-CRP antibody. The CRP concentration in blood serum is known to increase up to 1000-fold during acute inflammatory stress;[19,29,30] normal CRP values are below 5 μg mL^{-1}, while CRP level exceeds this threshold and reaches approximately 20 to 500 μg mL^{-1} in different inflammatory conditions. We found that CL intensity of luminol gradually decreased with the increasing concentration of CRP in the graphene-based CRET system (Figure 4A). The CRP concentration of 1 μg mL^{-1} caused luminol quenching efficiency of up to 72%. When plotted in a logarithmic scale, a linear relationship between CRP concentration and CL quenching was observed over a wide concentration range of 1−1000 ng mL^{-1} of CRP (Figure S5). This result indicates that CRP triggered anti-CRP antibody-conjugated graphene to undergo sandwich-type immunoreactions, serving as a bridge short enough for CRET to occur. In the case of BSA-blocked graphene without an anti-CRP antibody, no obvious signal change was observed even with the increasing CRP concentration, which supports the hypothesis that the CL quenching occurred through the recognition of CRP by specific interaction between the antigen and the antibody on graphene. When we tested the quenching efficiency of anti-CRP antibody-conjugated GO (instead of graphene), 26% quenching was obtained at the CRP concentration of 1 μg mL^{-1}. Considering that CRP is one of the key human blood serum markers for infections and inflammatory processes,[19] we further performed CRET-based CRP detection in human serum

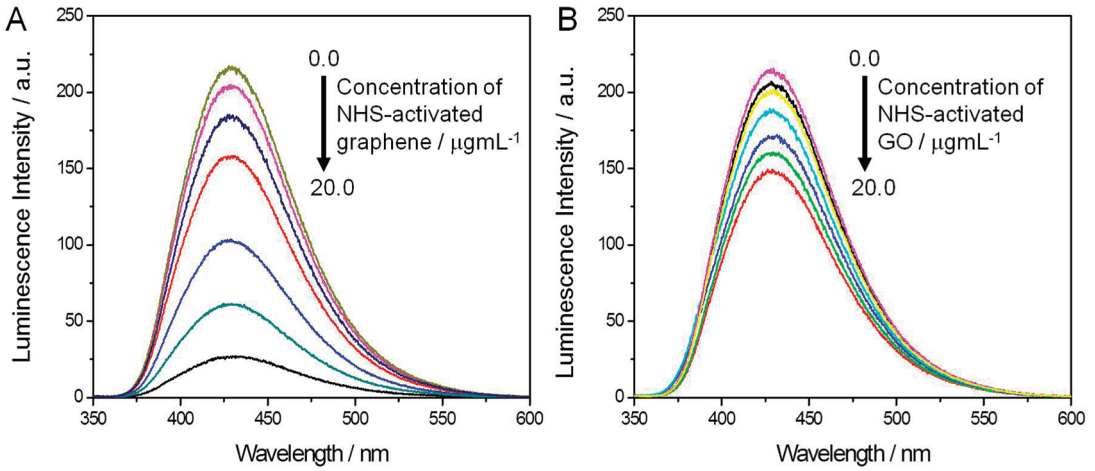

Figure 3. Chemiluminescence (CL) titration profile of luminol by (A) NHS-activated graphenes and (B) NHS-activated graphene oxide (GO) with concentrations ranging from 0 to 20 μg mL^{-1}. The increasing amount of the NHS-activated graphenes results in decreasing amount of free HRP and increasing amount of HRP immobilized on the graphene surfaces in the reaction solution, relatively. The degree of CL quenching at 430 nm reached approximately 91 and 36% with 20 μg mL^{-1} NHS-activated graphene or GO, respectively.

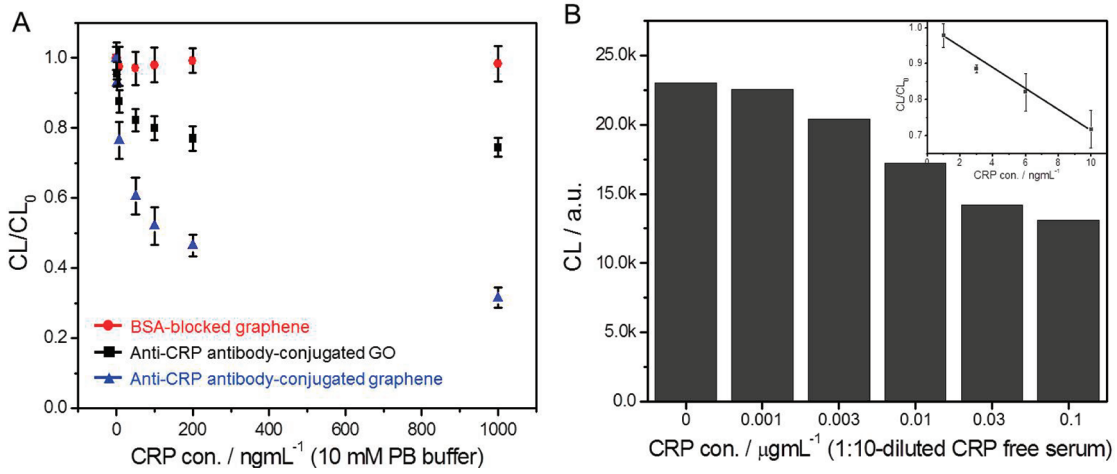

Figure 4. (A) Relative chemiluminescence (CL) emission intensity compared to that of original luminol (CL_0) after treatment with BSA-immobilized graphene, anti-CRP antibody-conjugated graphene oxide (GO), and anti-CRP antibody-conjugated graphene. (B) CL titration of luminol by CRP with concentrations ranging from 0 to 0.1 μg mL^{-1} in CRP-free human serum. The inset graph is a linear relationship at low CRP concentrations for the determination of LOD according to the following equation: $CL/CL_0 = -0.027$(CRP concentration) $+ 0.98$, $R^2 = 0.970$.

(Figure 4B). The limit of detection (LOD) of graphene-based CRET immnoassay was found to be 0.93 ng mL^{-1} for CRP in human serum. The CRET by CRP in human serum showed a similar quenching tendency to that by CRP in the buffer solution. For example, there was 47 and 43% CL quenching at the CRP concentration of 0.1 μg mL^{-1} for human serum sample and buffered sample, respectively. This indicates no interference of other biomolecules in the serum during the CRET process. We conducted an ELISA-based detection of CRP for comparison (Figure S6). The sensitivity of the graphene-based CRET platform was comparable to that of the ELISA-based assay, but the graphene-based CRET platform had significant advantage over ELISA by enabling homogeneous immunoassay without washing out unbound HRP-labeled secondary antibody. The graphene-based CRET platform allowed homogeneous immunoassay of specific target molecules without washing out unbound antibody or phase separation. Most often, sandwich-type immunoassays require the removal of unbound probes, such as fluorescent dyes or catalyst-labeled antibody, before signal readout to determine analyte concentration present in clinical and biological samples.[31]

CONCLUSION

We have demonstrated the graphene-based CRET platform for homogeneous immunoassay of CRP, a key marker for human inflammation and cardiovascular diseases. Anti-CRP antibody conjugated to graphene

nanosheets enabled the capture of CRP at the concentration above 1.6 ng mL^{-1}, which was verified by the gradual quenching of luminol CL. In the CRET platform, graphene played a key role as an energy acceptor, which was more efficient than GO, while luminol served as a donor to graphene, triggering the CRET phenomenon between luminol and graphene. The graphene-based CRET platform was successfully applied to the detection of CRP in human serum samples in the range observed during acute inflammatory stress. The graphene-based CRET system provides an efficient platform of immunoassay that does not require any removal of unbound antibody or phase separation, broadening the spectrum of graphene applications toward analytical biochemistry.

METHODS

Materials. C-reactive protein (CRP), anti-CRP polyclonal antibody, and HRP-labeled anti-CRP antibody were purchased from Invitrogen (Carlsbad, CA). Graphite powder, bovine serum albumin (BSA), *N*-(3-dimethylaminopropyl)-*N*-ethylcarbodiimde hydrochloride (EDC), and *N*-hydroxysuccinimide (NHS) were purchased from Sigma Aldrich (St. Louis, MO). All other reagents were of analytical reagent grade and used without further purification.

Preparation of Anti-CRP Antibody−Graphene and HRP−Graphene Conjugates. GO and water-soluble graphene were synthesized from natural graphite powder by the modified Hummers method.[20] Briefly, graphite powder (2 g) was mixed with $NaNO_3$ (1 g) and H_2SO_4 (45 mL) under stirring in an ice bath. Then, $KMnO_4$ (6 g) was slowly added with vigorous stirring at 35 °C. After 30 min, the mixture was gradually diluted, and a H_2O_2 solution was added in order to reduce the residual $KMnO_4$. The mixture was centrifuged at 15 000 rpm for 30 min, and the residue was washed out using deionized water. The obtained powder was redispersed in deionized water and exfoliated under sonication for about 1 h. GO powder was obtained after freezing and drying the suspension. Water-soluble, hydrothermally treated graphene was prepared according to the literature.[22] GO aqueous solution (0.5 mg mL^{-1}) was sealed within a Teflon autoclave and heated at 180 °C for 6 h. The resulting products, which contained hydrothermally treated graphene sheets, were redispersed in deionized water (0.5 mg mL^{-1}). To prepare the aryl diazonium salt solution, sulfanilic acid (50 mg) and sodium nitrite (19.8 mg) were dissolved in a 10 mL NaOH solution (0.25 wt %), which was added to a 10 mL HCl solution (0.1 N) in an ice bath under stirring. After reaction for 10 min, the aryl diazonium salt solution was added to a 50 mL graphene dispersion and was stirred vigorously for 2 h in an ice bath. After centrifugation and rinsing, the prepared graphene was readily dispersed in deionized water and formed a stable dispersion. For the synthesis of anti-CRP antibody−graphene conjugates, graphene (0.1 mg mL^{-1}) was activated by the addition of an aqueous mixture of EDC (2 mg mL^{-1}) and NHS (4 mg mL^{-1}). The mixture was gently mixed for 20 min at 25 °C. Then, anti-CRP antibody (1 mg mL^{-1}) in a phosphate buffer (10 mM, pH 8.0) was added to the solution. The samples were shaken at room temperature for 6 h. Remaining NHS-active sites of graphene were blocked with 2% bovine serum albumin (BSA) solution in a 50 mM phosphate buffer for 3 h. The solution was centrifuged at 13 000 rpm for 30 min at 4 °C to remove any unbound biomolecules. For HRP-immobilized graphene, graphene (0.1 mg mL^{-1}) was activated by EDC (2 mg mL^{-1}) and NHS (4 mgmL^{-1}) and centrifuged at 13 000 rpm. The NHS-activated graphene nanosheets (0−20 μg mL^{-1}) were then added to HRP solution (0.01 mg mL^{-1}). We conducted an ELISA-based detection of CRP to compare with the graphene-based CRET platform using the typical ELISA method. An ELISA plate was coated with anti-CRP antibodies, and after blocking with BSA, diluted CRP samples were added to each well and incubated for 2 h. Then, HRP-labeled anti-CRP antibodies were added and incubated for 1 h. A TMB Substrate Reagent Set (BD Biosciences, San Jose, CA) was used for the color development, and 0.16 N sulfonic acid was added to stop the reaction. The optical density at 450 nm was measured using a microplate reader TECAN Infinite M200 Pro (Tecan Group Ltd., Switzerland).

Characterization. For chemiluminescence measurements, the CRP sample and HRP-conjugated anti-CRP antibody were added to the anti-CRP antibody-conjugated graphene solution. After gentle shaking of the solution for 30 min, CL reaction buffer containing luminol/hydrogen peroxide (0.2 mM, each) was introduced into the solution. The final pH of this reaction mixture was 8.5. The CL spectra and intensity of the solution were recorded after 30 s using either RF-5301PC spectrofluorometer (Shimadzu, Japan) or a Victor3 microplate reader (Perkin-Elmer Inc., MA). In the case of CRP detection in human serum, CRP ranging from 0.1 to 10 μg mL^{-1} was spiked in a CRP-free human serum and then 10-fold diluted in a phosphate buffer (10 mM, pH 8.0). For AFM measurements, samples were placed on freshly cleaved mica and scanned using a Nanoscope III Multimode atomic force microscope (Digital Instruments Inc., Santa Barbara, CA) under ambient conditions. UV/vis absorption spectra of graphene and GO were recorded using a V-650 spectrophotometer (JASCO, Japan). FT-IR spectra of graphene and GO on silicon substrates were measured at a resolution of 2.0 cm^{-1} using a Bruker IFS66 V/S spectrometer coupled with a HYPERION 3000 microscope (Bruker Optics Inc., Germany). The CD spectrum of anti-CRP antibody and antibody-conjugated graphene was obtained using a J-810 instrument (JASCO, Japan).

Conflict of Interest: The authors declare no competing financial interest.

Acknowledgment. We thank anonymous reviewers for their input and advice in revising the manuscript. This study was supported by grants from the National Research Foundation (NRF) *via* NLRL program (2011-0028915), Converging Research Center (2009-0082276), National Research Laboratory (R0A-2008-000-20041-0), Intelligent Synthetic Biology Center of Global Frontier Project (2011-0031957), and Engineering Research Center (2012-0001175).

Supporting Information Available: UV/vis spectra, FT-IR spectrum, circular dichroism spectra, and chemiluminescence titration. This material is available free of charge *via* the Internet at http://pubs.acs.org.

REFERENCES AND NOTES

1. Wei, D.; Liu, Y. Controllable Synthesis of Graphene and Its Applications. *Adv. Mater.* **2010**, *22*, 3225–3241.
2. Huang, X.; Yin, Z.; Wu, S.; Qi, X.; He, Q.; Zhang, Q.; Yan, Q.; Boey, F.; Zhang, H. Graphene and Graphene Oxide: Synthesis, Properties, and Applications. *Adv. Mater.* **2010**, *15*, 3906–3924.
3. Yang, W.; Ratinac, K. R.; Ringer, S. P.; Thordarson, P.; Gooding, J. J.; Braet, F. Carbon Nanomaterials in Biosensors: Should You Use Nanotubes or Graphene?. *Angew. Chem., Int. Ed.* **2010**, *49*, 2114–2138.
4. Guo, Y.; Deng, L.; Li, J.; Guo, S.; Wang, E.; Dong, S. Hemin−Graphene Hybrid Nanosheets with Intrinsic Peroxidase-like Activity for Label-Free Colorimetric Detection of Single-Nucleotide Polymorphism. *ACS Nano* **2011**, *5*, 1282–1290.
5. Lu, G.; Park, S.; Yu, K.; Ruoff, R. S.; Ocola, L. E.; Rosenmann, D.; Chen, J. Toward Practical Gas Sensing with Highly Reduced Graphene Oxide: A New Signal Processing Method

To Circumvent Run-to-Run and Device-to-Device Variations. *ACS Nano* **2011**, *5*, 1154–1164.
6. Liu, Z.; Robinsin, R.; Sun, X. M.; Dai, H. PEGylated Nanographene Oxide for Delivery of Water-Insoluble Cancer Drugs. *J. Am. Chem. Soc.* **2008**, *130*, 10876–10877.
7. Balapanuru, J.; Yang, J.-X.; Xiao, S.; Bao, Q.; Jahan, M.; Polavarapu, L.; Wei, J.; Xu, Q.-H.; Loh, K. P. A Graphene Oxide–Organic Dye Ionic Complex with DNA-Sensing and Optical-Limiting Properties. *Angew. Chem., Int. Ed.* **2010**, *49*, 6549–6553.
8. Wang, H.; Zhang, Q; Chu, X.; Chen, T.; Ge, J.; Yu, R. Gaphene Oxide–Peptide Conjugate as an Intracellular Protease Sensor for Caspase-3 Activation Imaging in Live Cells. *Angew. Chem., Int. Ed.* **2011**, *50*, 7065–7069.
9. Kim, S.; Ku, S. H.; Lim, S. Y.; Kim, J. H.; Park, C. B. Graphene–Biomineral Hybrid Materials. *Adv. Mater.* **2011**, *23*, 2009–2014.
10. Swathi, R. S.; Sebastian, K. L. Distance Dependence of Fluorescence Resonance Energy Transfer. *J. Chem. Sci.* **2009**, *121*, 777–787.
11. Swathi, R. S.; Sebastian, K. L. Resonance Energy Transfer from a Dye Molecule to Graphene. *J. Chem. Phys.* **2008**, *129*, 054703.
12. Zhang, C.; Yuan, Y.; Zhang, S.; Wang, Y.; Liu, Z. Biosensing Platform Based on Fluorescence Resonance Energy Transfer from Upconverting Nanocrystals to Graphene Oxide. *Angew. Chem., Int. Ed.* **2011**, *50*, 6851–6854.
13. Swathi, R. S.; Sebastian, K. L. Long Range Resonance Energy Transfer from a Dye Molecule to Graphene Has $(\text{distance})^{-4}$ Dependence. *J. Chem. Phys.* **2009**, *130*, 086101.
14. Liu, M.; Zhao, H.; Quan, X.; Chen, S.; Fan, X. Distance-Independent Quenching of Quantum Dots by Nanoscale-Graphene in Self-Assembled Sandwich Immunoassay. *Chem. Commun.* **2010**, *46*, 7909–7911.
15. Ciruela, F. Fluorescence-Based Methods in the Study of Protein–Protein Interactions in Living Cells. *Curr. Opin. Biotechnol.* **2008**, *19*, 338–343.
16. Tu, D.; Liu, L.; Ju, Q.; Liu, Y.; Zhu, H.; Li, R.; Chen, X. Time-Resolved FRET Biosensor Based on Amine-Functionalized Lanthanide-Doped $NaYF_4$ Nanocrystals. *Angew. Chem., Int. Ed.* **2011**, *50*, 6306–6310.
17. Huang, X.; Li, L.; Qian, H.; Dong, C.; Ren, J. A Resonance Energy Transfer between Chemiluminescent Donors and Luminescent Quantum-Dots as Acceptors (CRET). *Angew. Chem., Int. Ed.* **2006**, *45*, 5140–5143.
18. Huang, X.; Ren, J. Gold Nanoparticles Based Chemiluminescent Resonance Energy Transfer for Immunoassay of Alpha Fetoprotein Cancer Marker. *Anal. Chim. Acta* **2011**, *686*, 115–120.
19. Blake, G. J.; Rifai, N.; Buring, J. E.; Ridker, P. M. Blood Pressure, C-Reactive Protein, and Risk of Future Cardiovascular Events. *Circulation* **2003**, *108*, 2993–2999.
20. Chen, W.; Yan, L.; Bangal, P. R. Preparation of Graphene by the Rapid and Mild Thermal Reduction of Graphene Oxide Induced by Microwaves. *Carbon* **2010**, *48*, 1146–1152.
21. Cai, X.; Tan, S.; Lin, M.; Xie, A.; Mai, W.; Zhang, X.; Lin, Z.; Wu, T.; Liu, Y. Synergistic Antibacterial Brilliant Blue/Reduced Graphene Oxide/Quaternary Phosphonium Salt Composite with Excellent Water Solubility and Specific Targeting Capability. *Langmuir* **2011**, *27*, 7828–7835.
22. Si, Y.; Samulski, E. T. Synthesis of Water Soluble Graphene. *Nano Lett.* **2008**, *8*, 1679–1682.
23. Bonanni, A.; Ambrosi, A.; Pumera, M. Nucleic Acid Functionalized Graphene for Biosensing. *Chem.—Eur. J.* **2012**, *18*, 1668–1673.
24. Zhou, J. C.; Chuang, M. H.; Lan, E. H.; Dunn, B.; Gillman, P. L.; Smith, S. M. Immunoassays for Cortisol Using Antibody-Doped Sol–Gel Silica. *J. Mater. Chem.* **2004**, *14*, 2311–2316.
25. Chen, Z.; Berciaud, S.; Nuckolls, C.; Heinz, T. F.; Brus, L. B. Energy Transfer from Individual Semiconductor Nanocrystals to Graphene. *ACS Nano* **2010**, *4*, 2964–2968.
26. Dong, H.; Gao, W.; Yan, F.; Ji, H.; Ju, H. Fluorescence Resonance Energy Transfer between Quantum Dots and Graphene Oxide for Sensing Biomolecules. *Anal. Chem.* **2010**, *82*, 5511–5517.
27. Liu, Y.; Liu, C.; Liu, Y. Investigation on Fluorescence Quenching of Dyes by Graphite Oxide and Graphene. *Appl. Surf. Sci.* **2011**, *257*, 5513–5518.
28. Zhang, X.; Xi, Q. A Graphene Sheet as an Efficient Electron Acceptor and Conductor for Photoinduced Charge Separation. *Carbon* **2011**, *49*, 3842–3850.
29. Ala-kleme, T.; Makinene, P.; Ylinen, T.; Vare, L.; Kulmala, S.; Ihalainen, P.; Peltonen, J. Rapid Electrochemiluminoimmunoassay of Human C-Reactive Protein at Planar Disposable Oxide-Coated Silicon Electrodes. *Anal. Chem.* **2006**, *78*, 82–88.
30. Review Criteria for Assessment of C-Reactive Protein (CRP), High Sensitivity C-Reactive Protein and Cardiac C-reactive protein (cCRP) Assays, 2005. Available at www.fda.gov/cdrh/oivd.guidance/1246.pdf.
31. Szmacinski, H.; Smith, D. S.; Hanson, M. A.; Kostov, Y.; Lakowicz, J. R.; Rao, G. A Novel Method for Monitoring Monoclonal Antibody Production during Cell Culture. *Biotechnol. Bioeng.* **2008**, *100*, 448–457.